

**Naval Research Laboratory**

Washington, DC 20375-5000

**AD-A253 347**



**NRL/MR/6385-92-7102**

# **Ultrasonic Characterization of Highly Attenuative Thick Composites**

**NARENDRA K. BATRA**

*Mechanics of Materials Branch  
Materials Science and Technology Division*

**July 24, 1992**

**DTIC  
ELECTE  
JUL 28 1992  
S B D**

**92 7 27 217**

**92-20301**



# REPORT DOCUMENTATION PAGE

*Form Approved*  
OMB No 0704-0188

Public reporting burden for this collection of information is estimated to average 1 hour per response, including the time for reviewing instructions, searching existing data sources, gathering and maintaining the data needed, and completing and reviewing the collection of information. Send comments regarding this burden estimate or any other aspect of this collection of information, including suggestions for reducing this burden, to Washington Headquarters Services, Directorate for Information Operations and Reports, 1215 Jefferson Davis Highway, Suite 1204, Arlington, VA 22202-4302, and to the Office of Management and Budget, Paperwork Reduction Project (0704-0188), Washington, DC 20503

<b>1. AGENCY USE ONLY (Leave blank)</b>	<b>2. REPORT DATE</b> July 24, 1992	<b>3. REPORT TYPE AND DATES COVERED</b>
---	--	---

<b>4. TITLE AND SUBTITLE</b> Ultrasonic Characterization of Highly Attenuative Thick Composites	<b>5. FUNDING NUMBERS</b> 62761N Task Area R561-544-500
--	---

<b>6. AUTHOR(S)</b> Narendra K. Batra	
--	--

<b>7. PERFORMING ORGANIZATION NAME(S) AND ADDRESS(ES)</b> Naval Research Laboratory Washington, DC 20375-5000	<b>8. PERFORMING ORGANIZATION REPORT NUMBER</b> NRL/MR/6385-92-7102
---	--

<b>9. SPONSORING / MONITORING AGENCY NAME(S) AND ADDRESS(ES)</b> Annapolis Detachment, Carderock Division Naval Surface Warfare Center Annapolis, MD 21402-5067	<b>10. SPONSORING / MONITORING AGENCY REPORT NUMBER</b>
--	---

<b>11. SUPPLEMENTARY NOTES</b>
--------------------------------

<b>12a. DISTRIBUTION / AVAILABILITY STATEMENT</b> Approved for public release: distribution unlimited.	<b>12b. DISTRIBUTION CODE</b>
---	-------------------------------

<b>13. ABSTRACT (Maximum 200 words)</b>  Thick composites manufactured from various fiber and matrix materials are being increasingly used for structural components. Conventional ultrasonic methods cannot be used to characterize nondestructively these highly attenuative materials. In this report we define the term "THICK" from a nondestructive evaluation (NDE) point of view which pertains to poor signal-to-noise (S/N) ratio of the received propagated signal in contrast to "THICK" as referred to the load-bearing limit. Ultrasonic nondestructive evaluation of such composites may involve analyzing the interaction of elastic waves with the physical properties of the material constituents. We developed ultrasonic transmission techniques which, when used in conjunction with specimens in the shape of wedges, steps or parallel plates, allow accurate measurement of attenuation and consequently evaluation of flaws in these materials. We will describe several ultrasonic methods developed for application to determine the variations in the attenuation to characterize thick composites.
--

<b>14. SUBJECT TERMS</b> Thick composites      Ultrasonic Composites              Nondestructive evaluation	<b>15. NUMBER OF PAGES</b> 43
	<b>16. PRICE CODE</b>

<b>17. SECURITY CLASSIFICATION OF REPORT</b> UNCLASSIFIED	<b>18. SECURITY CLASSIFICATION OF THIS PAGE</b> UNCLASSIFIED	<b>19. SECURITY CLASSIFICATION OF ABSTRACT</b> UNCLASSIFIED	<b>20. LIMITATION OF ABSTRACT</b> UL
--	---	--	---

## CONTENTS

ADMINISTRATIVE INFORMATION .....	iv
1. INTRODUCTION .....	1
2. NDE DEFINITION OF THICK COMPOSITES .....	2
3. ULTRASONIC METHODS .....	3
3.1 PULSE-TRANSMISSION TECHNIQUE .....	4
3.2 ULTRASONIC INTERFEROMETRIC TECHNIQUE .....	6
3.2.1 THEORY .....	7
3.2.2 EXPERIMENTAL SETUP .....	10
3.2.3 DATA ANALYSIS AND DISCUSSION .....	10
3.3 ULTRASONIC SPECTRAL ANALYSIS .....	12
3.3.1 THEORY .....	13
3.3.2 EXPERIMENTAL SET-UP AND RESULTS .....	15
4. SUMMARY .....	16
ACKNOWLEDGMENTS .....	17
REFERENCES .....	18

DTIC QUALITY INSPECTED 2

<b>Accession For</b>	
NTIS GRA&I	<input checked="" type="checkbox"/>
DTIC TAB	<input type="checkbox"/>
Unannounced	<input type="checkbox"/>
Justification _____	
By _____	
Distribution/	
<b>Availability Codes</b>	
Dist.	Avail and/or Special
A-1	

## **ADMINISTRATIVE INFORMATION**

**This task was done under the sponsorship of the Ship and Submarine Materials Block under the management of Mr. I. L. Caplan (DTRC 0115). This work was performed under the Program Element 62761N, Task Area R561-544-500 work unit 63-0261-00. This work was performed in the Materials Science and Technology Division (Code 6300), Naval Research Laboratory, Washington, DC.**

# ULTRASONIC CHARACTERIZATION OF HIGHLY ATTENUATIVE THICK COMPOSITES

## 1. INTRODUCTION

In recent years there has been tremendous progress in the development of new kinds of structural materials. It is now possible to combine together several desirable material properties which were often mutually exclusive to manufacture custom materials according to specific requirements. As an example, fiber-reinforced composites can be utilized in structural components which require high strength and light weight. Another reason for their popularity is the possibility of customizing their composition according to specific requirements. In fact one can use different kinds of fibers, or a different fiber layout and density, or a different material as a "matrix" according to the intended use and required properties. Possibilities range from highly ordered patterns (e.g., fiberglass woven cloth layers imbedded in epoxy) to randomly dispersed chopped fiber strands.

The variety of new materials already developed and the continuing trend towards highly specialized composites suggest that attention be devoted to the problem of their characterization. In fact, safety and economic considerations require reliable techniques for NDE of these new materials. It is also necessary to gain a good understanding of the effect of the different constituents and the role of the interfaces in order to predict properties with the goal of optimization, in view of specific requirements. A severe difficulty in the NDE of *many* of these newly developed materials is their high absorptivity with respect to the interrogating energy, e.g. ultrasonic waves. In fact, from NDE point of view, a material specimen can be defined thick or thin, not according to its physical thickness (as expressed e.g. in mm) but to its attenuation coefficient for the interrogating energy. This concept will be clarified further in Section 2.

There are a variety of problems which arise in the NDE of thick composites, depending on the physical properties of the material to be characterized, the nature of the flaws to be investigated and the special requirements for NDE specifications. In fact some NDE techniques are more suitable for certain materials than others. The possible flaws that occur in these materials can be overwhelming: there may be porosities, contaminants, inclusions, delaminations, moisture, fiber misalignment or breakage, matrix aging or inhomogeneities, etc. We wish to remark here that the term "flaw" may be misleading because some of the "flaws" may really be desirable features such as irregularities in the heterogeneous composition of the material. The signal due to the above detrimental flaws in thick composites is generally a small perturbation on the received signal which is in the noise level. For the purposes of detection of competing signals due to these flaws, one requires well-characterized high power transmitters and sensitive, high resolution receivers with appropriate signal processing. Among the "special requirements" which might affect the selection of a particular NDE technique over others, we may mention the availability and cost of the apparatus, its ease of use in the field, the time required for the job and the accessibility of the component to be inspected, as the deciding factor. A consideration which may prove to be of primary importance is whether the detection, location and characterization of the flaws in the component needs to be performed during the processing, fabrication or service phase of the work. Another important consideration is whether the data presentation and/or accept-reject criterion is qualitative or quantitative. In many cases the detection and/or evaluation of the severity of the flaw may be greatly eased by a complete automation of the NDE process.

It is important to assess and predict nondestructively the presence of irregularities, porosities, inclusions, and flaws, such as cracks and delaminations. For example, for composite materials such as fiber-reinforced polymers, it may be necessary to map ultrasonically the orientation and alignment of the fibers and to detect irregularities such as misalignment or heterogeneities of the fibers. In each case, one needs to measure variations in ultrasonic attenuation and/or phase velocity to assess the state of the material.

A large number of papers[1-19], applicable to the problem of characterizing composite materials already exist. In this report (Section 3), we shall limit ourselves to various ultrasonic techniques which we developed for application to the characterization of *highly attenuative* thick composites.

## 2. NDE DEFINITION OF THICK COMPOSITES

Specimens made of composite materials are usually thin in one or more dimensions (e.g. a few mm or a few cm thick). If the specimen is not of uniform thickness, the term "thick" generally refers to the load-bearing thick section. However from an NDE point of view what matters is the attenuating power of the specimen, with respect to the particular kind of interrogating energy used. Therefore the thickness of the material which can be inspected by NDE is restricted by the signal-to-noise ratio. This can be better understood with a few examples.

The amplitude of an acoustic wave propagating in a medium in the  $z$ -direction can be written as

$$A(z) = A_0 e^{-\alpha z} F(kz - \omega t) \quad (2.1)$$

where the attenuation coefficient  $\alpha$  (in nepers/cm or nepers/inch) depends on the material properties.  $A_0$  is amplitude at  $z = 0$ .  $F$  is a function of wave vector  $k$ , and angular wave frequency  $\omega$  and defines the shape of the interrogating ultrasonic energy.

Assuming that the noise level amplitude is given by  $A_{nl}$ , the equation

$$A(z_{max}) = A_{nl} \quad (2.2)$$

defines the maximum distance  $z_{max}$  for which a determination of  $A(z)$  can be relevant i.e., for the ultrasonic NDE of a material, the thickness  $d$  must be such that, for a given frequency, the amplitude of the transmitted signal  $A(d) > A_{nl}$ . If  $A(d) < A_{nl}$ , the material is defined as thick. Therefore, the decision of whether a material is thick or thin for the purposes of ultrasonic NDE depends on the acoustic properties of the material. For some highly heterogeneous composites

$$\alpha = 14.39 \text{ nepers/inch} = 125 \text{ dB/inch} \quad (2.3)$$

which means that, if input signal  $A_0 = 1 \text{ V}$ , the amplitude of the electric signal representing the acoustic wave on the oscilloscope, after a penetration of one inch is given by

$$A(1'') = 0.56 F(kz - \omega t) \mu V \quad (2.4)$$

which could be below the noise-level of many ultrasonic systems. However, if instead of ultrasound, a different type of interrogating energy, e.g. electromagnetic waves is used for NDE, the criterion for inspectable thickness would depend upon the electromagnetic properties of the material. All types of composites can be inspected by ultrasound whereas electromagnetic NDE techniques [20-22] are applicable only to the composites which are electrically conductive such as graphite/epoxy and may be able to inspect greater thickness. Moreover, these composites also do not have high acoustic absorption coefficient as compared, e.g., to kevlar/epoxy composites and thus, do not present S/N ratio problem. We restrict our ultrasonic study the latter class of composites, some which, depending upon the fiber layout, can have very high attenuation coefficient.

### 3. ULTRASONIC METHODS\*

Ultrasonic techniques offer several features which in many cases make them particularly convenient for NDE. They are safe, cost-effective and easy to use in different situations like in the laboratory or in the field. The high ultrasonic reflectivity of narrow defects such as cracks and their accessibility to ultrasound, even deep into the material may be an important factor for choosing an ultrasonic inspection over other NDE techniques. Interaction of these waves with the elastic properties of the composite can be used to detect and evaluate flaws.

Attenuation of ultrasonic waves propagating through a material is an important physical parameter. It gives us an indirect measure of the composition of the material. Certain constituents, such as fibers in the host matrix, can be added intentionally in order to create materials such as composites which are lighter and stronger than conventional structural materials, such as steel, aluminum and titanium, etc. In order to characterize these composite materials nondestructively, one needs to measure the attenuation and/or velocity of the propagating ultrasound through such materials and relate these acoustic parameters with the material properties or variation thereof. In this paper we concentrate on the measurement of attenuation in materials which are highly attenuative.

Ultrasonic pulse-echo systems have been widely used in recent years to measure the attenuation and ultrasonic group velocity with applications for tissue characterization in medicine [23-26] and material characterization in NDE [27-30]. Pulse-echo techniques require plane parallel specimens of low attenuation so that multiple echoes can be set up in the specimen. They do not measure absolute attenuation because of uncertainties due to reflection, transmission, and surface scattering, although losses due to these effects can be partially taken into account by processing multiple echoes. Due to a lack of spectral purity, they do not provide us with phase velocity, which is a more relevant quantity for the determination of elastic constants, stresses, texture, and material phases in the material. Ultrasonic attenuation due to impedance mismatch, surface roughness, and diffraction is generally irrelevant as far as the material characterization is concerned. The more relevant quantities are the attenuation due to absorption  $\alpha_{abs}$ , and to scattering  $\alpha_{sc}$ . Thus accurate and absolute values of the attenuation  $\alpha_{tot} = \alpha_{abs} + \alpha_{sc}$  and phase velocity can characterize a mac-

roscopically homogeneous material almost completely.

The difficulty of characterizing thick components lies in the fact that the detected signal is often masked by noise. It is not possible to observe multiple echoes in a plane parallel specimen due to high attenuation. Consequently one cannot determine the attenuation coefficient from the slope of the envelope of these multiple echoes. To overcome this difficulty, we developed various transmission techniques, as described in this section, to characterize these composites.

### 3.1 Pulse-Transmission Technique

There are several methods available for measuring the attenuation [31]. However, none of these techniques is suitable for highly attenuative materials. We demonstrate how the above difficulties of poor S/N can be circumvented by use of a ultrasonic pulse transmission technique in conjunction with a suitable choice of specimen geometry, such as steps or wedges (Fig. 1).

Whenever ultrasonic waves (elastic waves of high frequency) are propagated through a material, they lose energy through absorption and scattering. Scattering from the defects redistributes energy away from the direction of propagation while absorption converts the ultrasound energy into heat. Because of the loss of energy (attenuation), the amplitude,  $A$ , of a plane wave propagating in the  $z$ -direction can be written as:

$$A = A_0 e^{-\alpha z} \exp[i(2\pi ft - kz)] \quad (3.1.1)$$

where  $f$  is the frequency,  $k = \frac{2\pi}{\lambda}$  is the wave number, and  $\alpha$  is the total attenuation factor (usually expressed in dB/cm). In general,  $\alpha$  is a function of frequency and increases with frequency. Use of low frequency may increase the penetration depth but would limit us to poor resolution.

Equation (3.1.1) leads to an expression for determination of  $\alpha$  as

$$\alpha = \frac{1}{|z_1 - z_2|} \ln \left[ \frac{A_1(z_1)}{A_2(z_2)} \right] \quad \text{nepers/cm} \quad (3.1.2)$$

Recalling that  $A \text{ (dB)} = 20 \log \frac{A}{A_0}$ , we can rewrite  $\alpha$  as

$$\alpha = \frac{1}{|z_1 - z_2|} [A_1 \text{ (dB)} - A_2 \text{ (dB)}] \quad \text{dB/cm} \quad (3.1.3)$$

For this work we used specimens made of pure epoxy and fiber-reinforced composites. These composites consisted of fiberglass woven cloth layers imbedded in epoxy. There are also chopped fiberglass strands dispersed randomly in the epoxy matrix. One composite specimen consisted of a 14x7 cm plate with three equal steps of thickness,  $z_1 = 0.64 \text{ cm}$ ,  $z_2 = 1.01 \text{ cm}$  and  $z_3 = 1.53 \text{ cm}$  respectively. The other specimen consisted of an  $8^\circ$  right angle wedge with a base  $14.5 \times 7 \text{ cm}$ . A third specimen, in the shape of a wedge of  $13.8^\circ$ , was made out of epoxy. This specimen was used to check the validity of the experimental set-up (Fig. 2). A broadband pulse is transmitted normal

to the (x, y) face of a properly designed wedge shape specimen. Another properly aligned transducer receives the transmitted signal. The transmitting and receiving transducers are fixed relative to each other and scan together in the x-direction.

Fig. 3 shows the attenuation curve (dashed curve) for the first two steps ( $z_1 = 0.64\text{cm}$  and  $z_2 = 1.01\text{cm}$ ) of the composite specimen. We assume that the attenuation due to water is negligible. By averaging the amplitudes  $A_1(z_1)$  and  $A_2(z_2)$ , one obtains  $A_1 = -1\text{dB}$  and  $A_2 = -12\text{dB}$ , which yield  $\alpha = 31\text{dB/cm}$ . The oscillations in the attenuation are due to variations in the fiber concentration. Regions of lowest fibers concentration (mostly matrix) yield maxima and regions of the highest fiber concentration correspond to minima in the amplitude. By averaging the maxima and minima, one obtains  $\alpha_{lo} = 19\text{dB/cm}$  and  $\alpha_{hi} = 46\text{dB/cm}$ . If the fibers density were, at least locally, low, then  $\alpha_{lo}$  would approximate the attenuation coefficient for the matrix. However, randomly interdispersed chopped fibers in the matrix lead to deviation from this assumption. Attenuation curves for different values of  $y$  can be used to map the fibers layout and detect the regularities (lack of) in the fibers pattern and concentration.

To illustrate the utility of wedges for measurement of attenuation, we used an epoxy wedge specimen. The advantage of using the wedge is that the path of propagation can be changed continuously (instead of finite steps) from  $z=0$  to  $z_{max}$  at which the received signal is in the noise level. Since  $z = x \tan \theta$ , for a fixed  $\theta$ , the path of propagation  $z$  can be varied continuously by scanning the pair of transducers along the  $x$ -axis. The amplitude of the received signal as a function of  $z$  for a pure epoxy specimen is shown in Fig. 4a. (The scale on the left is nonlinear because the data system plots the data in this fashion). The curve is very nearly exponential, so the attenuation can be easily determined as its average slope (See Eq. 3.2.1). This yields  $\alpha = 9\text{dB/cm}$ . Figure 4b shows the perturbation on the attenuation due to scattering from a simulated flaw in this specimen. This perturbation on the attenuation curve (exponential) expected for an unflawed specimen can be used as a direct quantitative measure of the signature of the flaw.

Figure 5a shows how the above mentioned technique can be used to study a composite reinforced with tweed-like woven fiberglass lamina. As the transducers scan the specimen, the propagating ultrasound is intercepted alternatively by regions of cross-weave and the matrix. Due to strong scattering by cross-weave regions, the propagating ultrasound is highly attenuated and the received signal drops sharply. The oscillations show the periodicity of the cross-weave of the lamina in the matrix. This has a spatial period of approximately 6.5 mm over most of the specimen. This agrees well with the periodicity of the fiber weave measured optically. The exponential envelope (due to change in path of propagation) give the attenuation, which, in the region of cross-weave, is  $\sim 50\text{dB/cm}$  (lower envelope) and in the region of the matrix is  $\sim 30\text{dB/cm}$  (upper envelope). If there is any misalignment or in-homogeneity or gross local flaws, the attenuation curve will have local deviation from the exponential and, in the case of the composite specimen, lack of periodicity as is evident from Fig. 5b. For example the region  $z = 0.3$  to  $0.5\text{cm}$  (at  $x = 1.8$  to  $3.6\text{cm}$ ) is flawed for a particular value of  $y$ , when compared with a similar region for a different value of  $y$  (Fig. 5a). Thus this technique can be used to map the corresponding irregularities of the fibers and matrix flaws.

Thus we have demonstrated that it is possible to measure directly the attenuation in highly absorb-

ing materials by using a transmission technique and a properly designed specimen. The internal composition of the material is clearly depicted by the attenuation curve.

### **3.2 Ultrasonic Interferometric Technique**

In this section we will discuss how one can measure both attenuation and phase velocity simultaneously in highly attenuative materials [19] by analyzing the interference pattern between the incident and transmitted continuous ultrasonic waves. Our technique is somewhat similar to the one proposed for the measurement of attenuation and phase velocity in *liquids* by Sedlacek and Asenbaum [32]. They obtained an interference pattern by continuously changing the distance of propagation in the liquid by moving one of the transducers either closer to or farther from the other. Obviously, this can be done for propagation in a *liquid* but not in a solid.

The other techniques such as continuous wave (cw) ultrasonic spectroscopy [18], for simultaneous measurements of phase velocity and attenuation are applicable only to low-absorbing materials. Standing waves are set up in the plane parallel specimen acting as a resonant cavity. The quality factor  $Q$  of the resonances, defined [33] as the ratio between resonant frequency of a peak and its width, gives the attenuation, whereas frequency spacing between two consecutive resonances gives the phase velocity. This technique, however, is not applicable to heterogeneous materials or to materials with high acoustic attenuation. In fact, in these cases, multiple resonances are either missing or are very broad and overlapping, thus rendering the measurements meaningless, particularly when the acoustic parameters must be carefully evaluated to map variations in material properties.

These above difficulties may be overcome if we send an ultrasonic cw through the material and cross-correlate the signal from the transmitter with the signal from the receiver. An interference pattern, which contains all the information needed for the evaluation of the acoustical parameters, can be obtained by continuously varying the acoustical path. This can be done, in the simplest possible way, by studying a material specimen cut in the shape of a wedge. An alternative possibility, in the case of a material plate, is to send oblique cw's and sweep the incidence angle. While it is obvious that plates are of more practical interest than wedges, we prefer to devote the present discussion to the analysis of wedges. In fact, if the material is homogeneous, the only difference between waves entering wedges at different locations is their length of propagation path within the material (all other factors, such as boundary conditions, being identical); therefore, these specimens allow us to concentrate only on the analysis of interference effects, without having to worry about the angular dependence of reflection, refraction and mode conversion effects, which greatly complicate the physical picture. Consequently, one can determine absolute attenuation, since the boundary conditions for the incoming and outgoing cw's are the same at any given point. The refraction and reflection effects, occurring in the case of obliquely incident cw's in parallel plates, will be considered in a future research project.

Besides allowing the measurement of phase velocity and attenuation, our technique can also be used to detect and assess quantitatively material flaws and inhomogeneities. To demonstrate this, we drilled a hole in one of the specimens, normal to the direction of wave propagation and scanned the specimen in the usual fashion. The resulting interference pattern clearly shows the effect of the hole. A "signature of the defect" can be obtained by comparing the theoretical acoustical am-

plitude curve, expected for an unblemished specimen, with the experimental data. Our results suggest the possibility of an approach to the solution of the inverse problem of predicting the characteristics of the defect through an analysis of the experimentally measured acoustical amplitudes.

The theory and experimental setup used for the development of our technique are explained in 3.2.1 and 3.2.2. In Section 3.2.3, we discuss several methods for the analysis of the experimental data and illustrate them with results obtained for an unblemished epoxy specimen and for the same specimen after having drilled a hole in it.

### 3.2.1. THEORY

In order to characterize a homogeneous material, we fabricate a specimen of it in the shape of a wedge (Fig. 6) and place it in an ultrasonic immersion tank. The size of the specimen must be sufficiently small, so that it slides freely between the transducers, but long enough so that a large number of measurements can be performed. In our case, the distance  $l$  between the transducers was about 5 cm and the length of the specimen (x range) about 10 cm. Continuous longitudinal waves are propagated through the sample. We assume that the wedge angle  $\theta$  is small (in our case,  $\theta = 13.8$ ) and ignore, for the time being, all refraction and multiple reflection effects. The ultrasonic signals,  $S_T$  sent by the transmitter T, and  $S_R$  received by the transducer R, are given by [12]

$$S_T = F_T A_0 \cos(\omega t + \phi_0), \quad (3.2.1)$$

$$S_R = T_{12} T_{21} F_R A_0 \exp[-\alpha_1(l-y) - \alpha_2 y] \times \cos\left(\omega \left\{ t - \left[ \frac{(l-y)}{v_1} \right] - \frac{y}{v_2} \right\} + \phi_0\right), \quad (3.2.2)$$

where  $F_T$  and  $F_R$  are the response factors of the transmitter and of the receiver and associated electronics;  $T_{12}$  and  $T_{21}$  are the transmission factors between medium 1 (water) and medium 2 (material) and vice versa (they are constant since both the wedge angle  $\theta$  and the incidence angle are constant);  $\alpha_1$ ,  $\alpha_2$ ,  $v_1$ , and  $v_2$  are the attenuation coefficients and phase velocities in the two media;  $A_0$  is the amplitude of the incident cw;  $l$  is the (fixed) distance between the transducers; and  $y$  is the length of the propagation path of the cw in the material. By moving the wedge (or the transducers) parallel to the x axis,  $y$  can be varied. By choosing the origin of the x axis at the vertex of the wedge, we have

$$y = x \cdot \tan \theta, \quad (3.2.3)$$

where  $\theta$  is the angle of the wedge.

The two signals,  $S_T$  and  $S_R$ , are correlated through an electronic mixer (phase detector). The corresponding non-normalized cross-correlation factor is given by

$$\begin{aligned}\psi &= \int_{-T}^T S_T(t) S_R(t) dt \\ &= F_T F_R T_{12} T_{21} A_0^2 \exp[-\alpha_1(l-y) - \alpha_2 y] \mathfrak{S},\end{aligned}\quad (3.2.4)$$

where

$$\begin{aligned}\mathfrak{S} &= \int_{-T}^T \cos(\omega t + \phi) \cos\left[\omega\left(t - \frac{l-y}{v_1} - \frac{y}{v_2}\right) + \phi_0\right] dt \\ &= \frac{1}{2} \int_{-T}^T \cos\left[\omega\left(\frac{l-y}{v_1} + \frac{y}{v_2}\right)\right] dt \\ &\quad + \frac{1}{2} \int_{-T}^T \cos\left[2\omega t + 2\phi_0 - \omega\left(\frac{l-y}{v_1} + \frac{y}{v_2}\right)\right] dt.\end{aligned}\quad (3.2.5)$$

The cross-correlation time interval  $2T$  can be chosen arbitrarily large. If we choose

$$2T \gg \frac{2\pi}{\omega}, \quad (3.2.6)$$

the contributions of the second integral in Eq. (3.2.5) become negligible and

$$\mathfrak{S} = T \cos\left\{\omega\left[\frac{(l-y)}{v_1} + \left(\frac{y}{v_2}\right)\right]\right\}. \quad (3.2.7)$$

It then follows that

$$\psi = \psi_0 + C \exp(-\alpha y) \cos(by + \phi), \quad (3.2.8)$$

where

$$C = F_T F_R T_{12} T_{21} A_0^2 T \exp(-\alpha_1 l), \quad (3.2.9a)$$

$$\alpha = \alpha_2 - \alpha_1, \quad (3.2.9b)$$

$$b = \omega(s_2 - s_1), \quad (3.2.9c)$$

$$\phi = \omega l s_1, \quad (3.2.9d)$$

and  $s_i$  is the slowness given by

$$s_i = 1/v \quad (i = 1, 2). \quad (3.2.10)$$

In Eq. (3.2.8), a constant term  $\psi_0$  has been added to account for the arbitrary origin of the experimental acoustic amplitude scale.

Upon fitting Eq. (3.2.8) to the experimental data (see Sec. 3.2.3), we obtain the parameters  $\psi_0$ ,  $C$ ,

$\alpha$ ,  $b$ , and  $\phi$ , from which the phase velocity  $v_2$  and attenuation  $\alpha_2$  in the material can be easily deduced, since the corresponding quantities in water,  $v_1$  and  $\alpha_1$ , are well known. In fact, at room temperature 293.5 K,  $v_1 = 1483$  m/s, and since  $\alpha_1 \ll \alpha_2$ ,  $\alpha_1$  can be neglected. It follows that

$$\alpha_2 = \alpha_1 + \alpha = \alpha,$$

$$v_2 = \left( \frac{b}{\omega} + \frac{1}{v_1} \right)^{-1}. \quad (3.2.11a)$$

Let us now analyze the effect of refraction (Fig. 7). One side of the wedge is normal to the incident wave and, therefore, does not refract. The other side causes a deviation  $\theta - \theta_R$  from the original propagation direction, where  $\theta_R \leq \theta$  is the refraction angle at the wedge surface in water (we are assuming that  $v_2 > v_1$ ). Consequently, the receiving transducer must be rotated through an angle  $\theta - \theta_R$ , and the acoustic path increases by a distance

$$\begin{aligned} \Delta &= (l - l_0 - y) \left[ \frac{1}{\cos(\theta - \theta_R)} - 1 \right] \\ &= \frac{1}{2} (l - l_0 - y) (\theta - \theta_R)^2. \end{aligned} \quad (3.2.11b)$$

However, Eq. (3.2.8) still holds, but the values of the parameters  $C$ ,  $\alpha$ ,  $b$ , and  $\phi$  of Eq. (3.2.9) change slightly. In particular, when refraction effects are included,

$$\begin{aligned} \alpha_2 &= \alpha + \alpha_1 [1 + (\theta - \theta_R)^2/2] = \alpha, \\ v_2 &= \left\{ \frac{b}{\omega} + \frac{[1 + (\theta - \theta_R)^2/2]}{v_1} \right\}^{-1}, \end{aligned} \quad (3.2.12)$$

resulting in a small deviation in the values of  $\alpha_2$  and  $v_2$ . Here,  $\theta_R$  can be experimentally measured or, for better accuracy, obtained through Snell's law

$$\sin \theta_R / v_1 = \sin \theta / v_2$$

by implementing a Newton iteration procedure with Eq. (3.2.12).

Finally, we discuss briefly the effect of multiple reflections. Unless  $T_{12} = T_{21} = 1$ , there will be multiple reflections of the waves at both inside surfaces of the wedge and at T and R. A number of waves are thus generated, which add up to the basic signal  $S_R$ , given by Eq. (3.2.2). Assuming  $\theta \ll 1$  and considering only multiple reflections within the material wedge, we note that if the wave is reflected  $n$  times by each inside surface of the wedge, its acoustic path within the wedge is approximately  $(2n+1)y$ . Its amplitude is multiplied by a factor  $R^{2n}$ , where  $R$  is the reflection coefficient of the material, assumed to be the same at the two surfaces of the wedge. As a result, we obtain waves with cross-correlation factors still given by Eq. (3.2.8) but with different values of

the parameters and with a (slightly) variable transmission coefficient  $T_{21}$ . The interference of all these waves creates a slight modulation pattern, which needs to be explicitly taken into account for a better fitting of the experimental curves. Usually, the factor  $R^{2n}$  and the high attenuation in the material reduce the amplitude of the echoes so much that only doubly reflected waves ( $n=1$ ) need to be considered. Also, since the attenuation increases with the frequency, the modulation due to multiple reflections becomes negligible at higher frequencies.

### 3.2.2. EXPERIMENTAL SETUP

Before starting with the acquisition of the experimental data, the orientation of the specimen is adjusted such that the incident beam parallel to the  $y$  axis scans along the  $x$  direction in the wedge surface parallel to the  $x$ - $y$  plane. Broad-band transmitting (T) and receiving (R) transducers are mounted on the same bridge and scan together in the  $x$  direction and index in the  $z$  direction. Their spatial positions can be adjusted independently. They are aligned using pulse-echo as well as pitch-catch techniques (Fig. 2). The position and orientation of the transducer R are adjusted so that the received signal is maximum.

Once the orientations of specimen and transducers are fixed, the experimental setup is switched to the configuration, as shown in Fig. 8. Continuous waves of suitable frequency (in the range 2-20 MHz) are split into two parts. One portion of these waves is amplified and excites a broad-band immersion transducer (T). The other portion is fed into a phase-sensitive detector, whose dc output (proportional to the phase difference between input and output signals) is filtered, digitized, and transmitted to a VAX computer, under the control of a Tektronix desk top computer. The filtered signal can also be recorded on an  $x$ - $y$  chart recorder as a function of the propagation path  $y = x \cdot \tan\theta$  in the material.

### 3.2.3. DATA ANALYSIS AND DISCUSSION

Typical experimental cross-correlation curves for an unblemished epoxy specimen at different frequencies are shown in Fig. 9. They clearly show the exponential decay of the amplitude and the sinusoidal oscillations, as predicted by Eq. (3.2.8). By comparing the three curves obtained at different frequencies, we see that the attenuation  $\alpha$  increases with the frequency, as expected. We also notice that the intervals between successive peaks become progressively smaller at higher frequencies, as predicted by Eq. (3.2.9c), which shows that the coefficient  $b$  of Eq. (3.2.8) is proportional to the frequency.

For a quantitative fitting of the experimental data and consequent extraction of the parameters of interest, we used three different methods. With the first method, we obtain the five parameters  $\psi_0$ ,  $C$ ,  $\alpha$ ,  $b$ , and  $\phi$  by fitting five points, which can be conveniently chosen, such as  $y_1 = 0$  (theoretically, at the edge of the wedge but, in practice, sufficiently apart to avoid diffraction from the edge), the first two maxima, first minimum, and one more maximum near the end of the  $y$  range (see Fig. 10). By substituting in Eq. (3.2.8) and noting that  $\cos(by + \phi)$  is equal to 1 at the maxima and to -1 at the minima, one easily obtains

$$b = \frac{2\pi}{(y_4 - y_2)}, \quad (3.2.13a)$$

$$\psi_0 = (\psi_2 + 2\psi_3 + \psi_4)/4, \quad (3.2.13b)$$

$$\alpha = \log [(\psi_2 - \psi_0) / (\psi_5 - \psi_0)] / (y_5 - y_2), \quad (3.2.13c)$$

$$\phi = \text{atan}(-\alpha/b) - by_2 + n\pi, \quad n = 0, \pm 1, \pm 2, \dots, \quad (3.2.13d)$$

$$C = \frac{(\psi_1 - \psi_0)}{\cos \phi}. \quad (3.2.13e)$$

In Eq. (3.2.13d),  $n$  must be chosen even or odd, as necessary to make  $C$ , in Eq. (3.2.13e), positive.

Equations (3.2.13) and (3.2.11a) or (3.2.11b) allow us to evaluate, in a very simple fashion, the attenuation  $\alpha$ , and phase velocity  $v_2$  in the material. The accuracy may not be too good, however, since the experimental curve is determined by a large but finite number of points, due to the finite step of the increment in the  $x$  direction (0.025 mm). Although the experimental errors are rather small (on the average, much less than 1%), it may be difficult to pinpoint the precise location of the maxima (or minima).

A second method for the analysis of the experimental data consists of considering all the maxima and minima. In this way, it is possible to reduce the error in the evaluation of the interval between two successive maxima by averaging through many such intervals. This method, however, requires more manipulation of data and, therefore, is much more time-consuming. To have it completely computerized is possible, but not trivial, since local random fluctuations may be interpreted as maxima or minima, thus compromising the reliability of the results. This method has been applied for the data analysis contained in Ref. 19, yielding standard deviation for the phase velocity of the order of 0.5%.

For the work, we adopted a different, but much more powerful method, which consists of least-squares fitting *all* the (about 500) experimental points to the theoretical curve given by Eq. (3.2.8). In this way, all the experimental points (rather than only a few selected ones) contribute to the evaluation of the parameters of interest. A computer program written for the purpose takes only a few seconds to run on a Digital VAX 11/780 for each case considered. In the program, a dichotomic procedure can be used very efficiently, although some care must be exercised to insure convergence to the global minimum (of the sum of the deviations square), rather than to a local one. With this method, we have obtained an accuracy, in the determination of  $v_2$ , of better than 0.1%. This accuracy could be further increased by digitizing the experimental acoustic amplitude measurements over a wider range (in our case, the range was 0-255), thus reducing accordingly the experimental errors.

Although, in principle, the same accuracy can also be achieved in the evaluation of the attenuation, in practice the standard deviations here are much larger, because of possible losses due to surface roughness, cutting of the wedge surface that is not perfectly straight, and local inhomoge-

neities. On the other hand, the attenuation measurement can be used to detect these or other irregularities. It should also be pointed out that, unless they are properly taken into account, (multiple) internal reflections can be a large source of error in the determination of the attenuation, especially at low frequencies.

In order to demonstrate the applicability of our technique to the detection of defects, we have drilled a hole (of 0.25-cm diam.) in one of our epoxy specimens, normal to the cw propagation direction, and measured the corresponding acoustical amplitude pattern. The result is shown in Fig. 11. By comparing Fig. 11 with Fig. 9(a), we can very clearly observe the effect of the hole in the region between  $y = 0.3$  and  $0.5$  cm. The effect can be best observed by subtracting the experimental acoustic amplitude from the theoretical least-squares fitted curve. For an even better representation, after having determined where the defect lies, one can repeat the least-squares fitting excluding the range affected by the defect. In this way, one obtains values of  $\alpha_2$  and  $v_2$  that are not affected by the presence of the defect. Also, by subtracting the experimental data, one obtains the true "signature" of the defect [Fig. 12(b)]. For comparison, Fig. 12(a) shows the random fluctuations obtained when the defect is absent. Other smaller holes (down to 0.39 mm) were drilled elsewhere in the specimen; their signatures were noticeable, although much less conspicuous. If better precision of measurements were available, we could have better representations of these defects and consequently reduce the background noise. By accumulating results like Fig. 12(b) for different kinds and sizes of defects, one can learn to solve the inverse problem of detecting and quantitatively assessing an unknown defect.

Beside the information contained in the envelope of the curve of Fig. 12(b), the periodicity of the oscillations and the phase shift found through the defect range can provide information about phase velocity changes in the defect region. In our specimen, we have found a decrease, albeit very small, in the phase velocity, possibly due to the acoustoelastic effect [34] of the residual stress introduced by the drilling of the hole. The effect, however, was too small (only slightly larger than the standard deviation for  $v_2$ ) to justify a quantitative analysis.

### 3.3 ULTRASONIC SPECTRAL ANALYSIS

The pulse-echo [35] technique which is commonly used in measurements of attenuation is inadequate, due to lack of multiple echoes, as seen in acoustically transparent parallel plate metallic specimens. In the previous section we used wedge-shaped specimens to measure attenuation in these materials, using an ultrasonic interferometric technique. Such a technique, however, requires a special geometry of the specimen and therefore can be of limited use. The attenuation in a material is loss in energy due to absorption and scattering. In general, as pointed out earlier, the signal-to-noise ratio is very poor and, depending on the thickness of the specimen, one may not be able to observe a transmitted pulse. One can determine the attenuation from this pulse using a substitution method [36] or by time delay spectroscopy [37]. Neither of these methods yields information about the frequency dependence of the attenuation, unless by sweeping the frequency.

The attenuation of propagating ultrasound through heterogeneous materials such as fiber-reinforced epoxy composites containing chopped fibers with random orientation is predominantly

due to scattering from the fibers as well as from discontinuities such as pores and is consequently frequency dependent. In this section, we determine the frequency dependent attenuation from the downshifted spectra of the transmitted broadband wavepacket. Such a technique, first used for medical ultrasound, can be very useful for characterization of acoustically very lossy composites, because spectral shifts for such materials can be particularly significant. It also allows use of parallel plate specimens. Analytical models and experimental results are presented in sections (3.3.1) and (3.3.2).

### 3.3.1 THEORY

An ultrasonic wave propagating through an inhomogeneous material suffers losses in energy due to scattering, which can be caused by spatial variations in absorption properties or in material density and/or in wave velocity. We assume that the attenuation in a signal propagating through such a dispersive material is frequency dependent and is given by

$$\alpha(f) = \alpha_0 f^n \quad (3.3.1)$$

where  $\alpha_0$  and  $n$  are material characteristics.

We briefly review and extend the mathematical analysis of Narayana and Ophir [38]. Let us consider a rectangular burst of amplitude  $A_0$ , duration  $T_0$  and center frequency  $f_0$ , incident on a plane parallel plate of composite material. Such a pulse in the time domain can be written

$$\begin{aligned} h(t) &= A_0 \cos(2\pi f_0 t) \quad \text{for } |t| < T_0/2 \\ &= 0 \quad \text{for } |t| > T_0/2 \end{aligned} \quad (3.3.2)$$

Its Fourier transform [39] is given by

$$\begin{aligned} H(f) &= A_0^2 T_0 [Q(f+f_0) + Q(f-f_0)] \\ \text{where } Q(f) &= \frac{\sin(\pi T_0 f)}{\pi T_0 f} \end{aligned} \quad (3.3.3)$$

The frequency spectrum of the incident pulse is then given by

$$I(f) = \frac{A_0^2 T_0 \sin \pi T_0 (f-f_0)}{\pi T_0 (f-f_0)} \quad (3.3.4)$$

When such a pulse is transmitted through an attenuating material, both the amplitude of its center peak and its bandwidth decrease. Further, if the attenuation is frequency dependent (assume  $n > 1$ ), then the amplitude at higher frequencies is attenuated more than at lower frequencies. Consequently there is an apparent frequency shift of the peak. The attenuation of the material can be determined from this shift in frequency of the central maximum (peak).

We describe the medium of propagation by

$$M(f) = e^{-\alpha(f)z} \quad (3.3.5)$$

where  $\alpha(f)$  is given by Eq. (3.3.1) and  $z$  is path of propagation in the lossy material. The spectrum of the signal transmitted through the material is given by

$$T(f) = I(f) \otimes M(f) \quad (3.3.6)$$

In order to find the shift in center frequency  $f_0$ , we set

$$\left. \frac{dT(f)}{df} \right|_{f=f_c} = 0 \quad (3.3.7)$$

where  $f_c$  is the center frequency of the received wavepacket, i.e.

$$\left. \frac{d}{df} \left[ \frac{A_0^2 T_0 \sin 2\pi T_0 (f - f_0)}{2\pi T_0 (f - f_0)} e^{-\alpha_0 f z} \right] \right|_{f=f_c} = 0 \quad (3.3.8)$$

Upon simplification, one obtains,

$$\cos \pi T_0 (f_c - f_0) - \frac{\sin \pi T_0 (f_c - f_0)}{\pi T_0 (f_c - f_0)} [n \alpha_0 z f_c^{n-1} (f_c - f_0) + 1] = 0 \quad (3.3.9)$$

Let

$$x = (f_c - f_0) \pi T_0 \quad (3.3.10)$$

then Eq. (3.3.9) can be written as

$$n \alpha_0 z f_c^{n-1} = \frac{\pi T_0}{z} \left[ \frac{1}{\tan x} - \frac{1}{x} \right] \quad (3.3.11)$$

Let

$$Y = \left[ \frac{1}{\tan x} - \frac{1}{x} \right] \quad (3.3.12)$$

then

$$n\alpha_0 f_c^{n-1} = \frac{\pi}{z} Y T_0 \quad (3.3.13)$$

or

$$\alpha_0 = \frac{\pi}{z} \frac{Y T_0}{n f_c^{n-1}} \text{ nepers cm}^{-1} \text{ MHz}^{-n} \quad (3.3.14)$$

For the purpose of analyzing the experimental data, one can write Eq. (3.3.14) in a linear form by taking the logarithm of both sides. From this linear relationship, one can determine  $n$  or  $\alpha_0$ , by measuring  $f_c$ , for two different values of  $T_0$  or  $f_0$ . The attenuation in the material at frequency  $f_0$  is then determined by

$$\alpha = 8.686\alpha_0 f_0^n \quad \text{dB cm}^{-1} \quad (3.3.15)$$

where the material parameters  $\alpha_0$  and  $n$  have been determined by the procedure outlined above.

### 3.3.2 EXPERIMENTAL SET-UP AND RESULTS

Figure 13 shows the experimental set up. Two matched 2.25 MHz broadband immersion transducers were used to transmit and receive a rectangular toneburst through a parallel plate specimen (70 mm x 40 mm x 8 mm). A rectangular toneburst of a given frequency is generated by gating a continuous wave rf signal with a very precise rectangular pulse. The amplified toneburst is used to excite the transmitter. Both the incident and the received signals are monitored on a scope to make sure that the amplifier gains are proper and the shape of these pulses is rectangular as desired.

First, the transducers are aligned without the specimen and the spectrum of the pulse propagating through water is analyzed. The effect of amplifier gains on the shape and peak frequency of the pulse transmitted through water is studied by attenuating the incident pulse (Fig. 14). It is clear that the peak frequency does not shift as a function of artifacts such as amplifier gain etc. It is expected this will be the case even in the presence of the specimen.

Figures 15 (a-c) show the changes to the center frequency of the peak for various durations of the incident rectangular toneburst. These effects are caused by attenuation in the specimen. For each  $T_0$ , the upper trace shows the spectrum of the pulse propagated through water. When the specimen is inserted between the transducers, three things happen: (1) the amplitude of the peak drops, (2) the position of the center peak is downshifted, and (3) the bandwidth of the center peak decreases. The incident pulse for water as specimen is attenuated by 20 dB, to keep its spectrum on the page along with that of the composite material for comparison and analysis. As  $T_0$  increases, e.g. from broadband to narrowband (quasi-continuous waves), the shift in the frequency decreases, as one would expect qualitatively. But the number of sidelobes also increases as  $T_0$  increases from 6  $\mu$ sec

to 11  $\mu$ sec. Using these measured values of  $f_0$  and  $f_c$  in Eq. (3.3.14), we find from a set of simultaneous equations, a value of  $n = 58$ , which is rather high. But it indicates that, due to various heterogeneities present in the specimen, the attenuation is mostly due to scattering and depends very strongly upon frequency. The amount of attenuation due to scattering at 2.7 MHz was determined to be about 16 to 20 dB/cm depending upon the location in the specimen. The total attenuation in these materials determined earlier [40] by using a wedge specimen was found to be  $\sim 32$  dB/cm. From the above data, using a substitution technique analysis, the total attenuation turns out to be 27 dB/cm, which agrees well with previous results. This variation of 15% in the measured value can easily be caused by heterogeneities in the material. By measuring the frequency dependent component of the attenuation, it is demonstrated that in these materials the attenuation is indeed dominated by losses in energy due to scattering.

#### 4. SUMMARY

In this report we have shown how to characterize highly attenuative materials which can barely transmit ultrasound. The type of energy used for nondestructive evaluation of thick composites must be able to penetrate through the thickness of the specimen under interrogation. One needs a sensitive receiver and good signal processing for extracting signals due to a flaw. A specimen which is "thick" (i.e., poor signal/noise ratio) for one type of NDE method may not be "thick" for another NDE method, provided the method is capable of evaluating the specific flaws encountered.

We have demonstrated that it is possible to measure the attenuation accurately in highly absorbing materials by using a transmission technique and a properly designed specimen. The internal composition of the material is clearly depicted by the attenuation curve.

We have discussed the application of ultrasonics to characterize thick composites. Ultrasonic techniques based on propagation of elastic waves through the material are generally applicable to all types of highly attenuative materials whereas eddy current techniques are applicable only to electrically conducting composites such as graphite-epoxy. The data acquired for the various types of flaws can be transformed into computer-generated images of spatial variation of selected material properly.

We proposed an ultrasonic technique for the simultaneous determination of the phase velocity and attenuation, which can be used for the characterization of highly attenuative materials. The technique is based on the interference between the incident (reference) cw signal and the signal after propagation through the material. The interference pattern, obtained when the acoustical path is continuously varied, contains all the information necessary to evaluate the phase velocity and attenuation of the material and any eventual anomaly or irregularity in the material. In order to obtain a continuous variation of acoustical path without the complications arising from changing boundary conditions, we fabricated a material specimen in the shape of a wedge and scanned it in the direction normal to its edge. Characteristic interference patterns have been obtained from the acoustical amplitude at different frequencies. Several methods were adopted for the analysis of the experimental data. We have found that a least-squares fit to the theoretically predicted curve can be a very efficient procedure, which allows the determination of the phase velocity with an accuracy of better than 0.1%. Larger standard deviations are found for the attenuation, but they reflect physical characteristics of the specimen, such as inhomogeneities or imperfect surface. By

drilling a hole through the specimen, normal to the direction of propagation of the cw, we simulated the presence of a defect and showed that our technique is quite capable of detecting it. By subtracting the experimental acoustic amplitudes from the theoretical curve, we have shown that it is possible to obtain a distinctive track of the defect, which can be used for its quantitative assessment, once a sufficient number of signatures of defects of different size and shape have been collected as reference.

Measurement of attenuation by frequency shift in the spectra of a transmitted wavepacket of known shape allows use of parallel plate specimens. It is a viable technique for characterization of such materials. Analysis and technique could be extended to other types of wavepacket and specimens of other composite materials, in which scattering of the ultrasound is the dominant cause of attenuation. The model should be extended to correlate the frequency shift in the side lobes of a transmitted pulse. It is expected that side lobes will have higher frequency shifts and may give increased accuracy.

## **ACKNOWLEDGMENTS**

The work reported here was conducted in the Nondestructive Evaluation Section of the Naval Research Laboratory under the sponsorship of Ships and Submarine materials Block Program managed by Mr. Ivan L. Caplan, Code 0115, Annapolis Detachment, Carderock Division, Naval Surface Warfare Center, Annapolis, MD 21402 (formerly David Taylor Research Center (DTRC)). The author thanks Mr. Ivan L. Caplan and Mr. Robert DeNale (Code 2815) for their interest and sponsorship of this project. Parts of this report are taken from the following published papers\*.

N.K. Batra, "Attenuation Measurement in Highly Absorbing Materials", Proceedings of 34th Defense Conference on Nondestructive Testing, pp 197-203 (1985).

N.K. Batra and P.P. Delsanto, J. Acoust. Soc. Am. 85, 1167 (1989).

N.K. Batra, "Ultrasonic Spectral Analysis for Characterization of Composites," Review of Progress in Quantitative Nondestructive Evaluation, Vol. 8B, pp. 1527-1533 (1989).

N.K. Batra, H.H. Chaskelis and P.P. Delsanto, "Nondestructive Evaluation of Thick Composites: A Review", Thick Composite Technology, 36th Sagamore Army Research Conference Proceedings October 23-26, 1989, Plymouth, MA, pp 239- 255.

## REFERENCES

1. J.L. Rose, Y.H. Jeong and M.V. Avioli, "Utility of a Probability Density Function and F-maps in Composite Material Inspection," *Experimental Mechanics* 22(4) (1982).
2. J.L. Rose, V.B. Nestleroth, and K. Balasubramanian "Utility of Feature Mapping in Ultrasonic Nondestructive Evaluation," *Ultrasonics*, 26, pp. 124-131 (1988).
3. V. B. Nestleroth, J. L. Rose, M. Bashram and K. Balasubramanian, "Physically Based Ultrasonic Feature Mapping for Anomaly Classification in Composite Materials," *Materials Evaluation* 43(5) (1985).
4. Wolfgang Sachse, B. Castagnede, I. Grabec, K.Y. Kim and R.L. Weaver, "Recent Developments in Quantitative Ultrasonic NDE of Composites," *Ultrasonics*, 28, 97-104 (1990).
5. W. Sachse and K.Y. Kim "Quantitative AE and Failure Mechanics of Composite Materials," *Ultrasonics* 25, 195-203 (1987).
6. R.L. Weaver, W. Sachse, and L. Niu, "Transient Ultrasonic Waves in a Viscoelastic Plate: I. Theory; II. Applications to Materials Characterization," *J. Acoust. Soc. Am.*, 6 2255-2267 (1989).
7. D. Yanwu, S. Yongchen, W. Zhigang, Z. Jun, and Q. Yunqiu, *J. Pure Appl. Ultrason. (India)* 8, 96 (1986).
8. L.S. Wilson, D.E. Robinson, K.A. Griffiths, A. Manoharan, and B.D. Doust, *Ultrason. Imag.* 9, 236 (1987).
9. P.D. Edmonds and C.L. Mortensen, in "Proceedings of the IEEE 1987 Ultrasonics Symposium," Denver, 14-16 October 1987 (IEEE, New York, 1987), Vol. 2. p. 915.
10. E.P. Papadakis, in "Physical Acoustics," edited by W.P. Mason and R.N. Thurston (Academic, New York, 1976), Val. 12, p. 277.
11. L.C. Lynnworth, E.P. Papadakis and K.A. Fowler, in "International Advances in Nondestructive Testing," edited by W.J. McGonnagle (Gordon and Breach, London, 1977), Vol. 5, p. 71.
12. W. Sachse and N.N. Hsu, in "Physical Acoustics," edited by W.P. Mason and R.N. Thurston (Academic, New York, 1979), Vol. 14, p. 277.

13. E.P. Papadakis, *J. Test. Eval.* 12, 273 (1984).
14. T.D.K. Ngoc, K.R. King, and W.G. Mayer, *J. Acoust. Soc. Am.* 81, 874 (1987).
15. J.L. Rose, P. Karpur and V.L. Newhouse, *Mater. Eval.* 46, 114 (1988).
16. N.K. Batra and T.P. Graham, "Measurement of Moisture in Hygrothermally Degraded Fiber-Reinforced Epoxy Composites by Continuous Wave (CW) Nuclear Magnetic Resonance (NMR)," *British J. of NDT*, pp. 21-23 (1983).
17. N.K. Batra, H.H. Chaskelis, and P.P. Delsanto, in *Proceedings of the IEEE 1985 Ultrasonic Symposium*, edited by B.R. McAvoy, San Francisco, 16-18 October 1985 (IEEE, New York, 1985), Vol. 2, p. 975.
18. N.K. Batra and H.H. Chaskelis, *Non-Destr. Testing Communications* 2, 65 (1985).
19. N.K. Batra and P.P. Delsanto, in *Review of Progress in Quantitative Nondestructive Evaluation*, edited by D.D. Thompson and D.E. Chimenti (Plenum, New York, 1987), Vol. 6A, p.491.
20. Hugo L. Libby, *Introduction to Electromagnetic Nondestructive Test Methods*, Wiley Interscience New York, 1971.
21. Paul McIntire and Michael L. Mester, Eds., *Nondestructive Testing Handbook, Second Edition, Vol. 4, Electromagnetic Testing*, American Society for Nondestructive Testing, Inc. (1986).
22. Susan N. Vernon, "Eddy Current Nondestructive Inspection of Graphite Epoxy Using Finite Cup Core Probes," in: *Tech. Report NSWC TR 87-148*, Naval Surface Warfare Center, Silver Spring, MD 20903. (1980).
23. D. Yanwu, S. Yongchen, W. Zhigang, Z. Jun, and Q. Yunqiu, *J. Pure Appl. Ultrason. (India)*, 8, 96 (1986).
24. J.H. Choi and J.S. Choi, in *Proceedings of TENCON 87: 1987 IEEE Region 10 Conference on "Computers and Communications Technology Toward 2000,"* Seoul, Korea, 25-28 August 1987 (IEEE, New York, 1987), Vol.3, p. 1322.
25. L.S. Wilson, D.E. Robinson, K.A. Griffiths, A. Monoharan, and B.D. Doust, *Ultrason. Imag.* 9, 236 (1987).
26. P.D. Edmonds and C.L. Mortensen, in *Proceedings of the IEEE 1987 Ultrasonics Symposium*, Denver, 14-16 October 1987 (IEEE, New York, 1987), Vol. 2, p.915.

27. E.P. Papadakis, in *Physical Acoustics*, edited by W.P. Mason and R.N. Thurston (Academic Press, New York, 1976), Vol. 12, p.277.
28. L.C. Lynnworth, E.P. Papadakis, and K.A. Fowler, in *International Advances in Nondestructive Testing* edited by W.J. Mc Gonnaghe (Gordon and Breach, London, 1977), Vol. 5, p.71.
29. W. Sachse and N.N. Hsu, in *Physical Acoustics*, edited by W.P. Mason and R.W. Thurston (Academic, New York, 1979), Vol. 14, p. 277.
30. E.P. Papadakis, *J. Test. Eval.* 12, 273, (1984).
31. M. A. Breazeale et al, "Methods of Experimental Physics," P.D. Edmonds, ed. (Academic Press, New York, 1981), 19, pp. 67-135.
32. M. Sedlacek and A. Asenbaum, *J. Acoust. Soc. Am.* 62, 1420 (1977).
33. D.I. Bolef and J.G. Miller, in *Physical Acoustics*, edited by W.P. Mason and R.N. Thurston (Academic, New York, 1971), Vol. 8, p. 95.
34. Y.H. Pao, W. Sachse, and H. Fukuoka, in *Physical Acoustics*, edited by W.P. Mason and R.N. Thurston (Academic, New York, 1984), Vol. 17, p.61.
35. R. Truell, C. Elbaum, and B.B. Chick, "Ultrasonic Methods in Solid State Physics," Academic Press, New York, 1969, Chapter 2.
36. D.K. Hsu and S.M. Nair, "Evaluation of Porosity in Graphite-Epoxy Composite by Frequency Dependence of Ultrasonic Attenuation," in: *Review of Progress in Quantitative Non-Destructive Evaluation*, Vol. 6, edited by D.O. Thompson and D.E. Chimenti, Plenum Press, New York (1987), pp. 1185-1193.
37. P.M. Gammell, "Ultrasonic Characterization of Highly Attenuating Materials with Time Delay Spectroscopy," *Proceedings of the 15th Symposium on Nondestructive Evaluation*, San Antonio, TX (1985).
38. P.A. Narayana and J. Ophir, "Spectral Shifts of Ultrasonic Propagation: A Study of Theoretical and Experimental Models," *Ultrasonic Imaging* 5, 22-29 (1983).
39. E. Oran Brigham, "The Fast Fourier Transform," Prentice-Hall, NJ (1974).
40. N.K. Batra and P.P. Delsanto, *J. Acoust. Soc. Am.* 85, 1167 (1989).

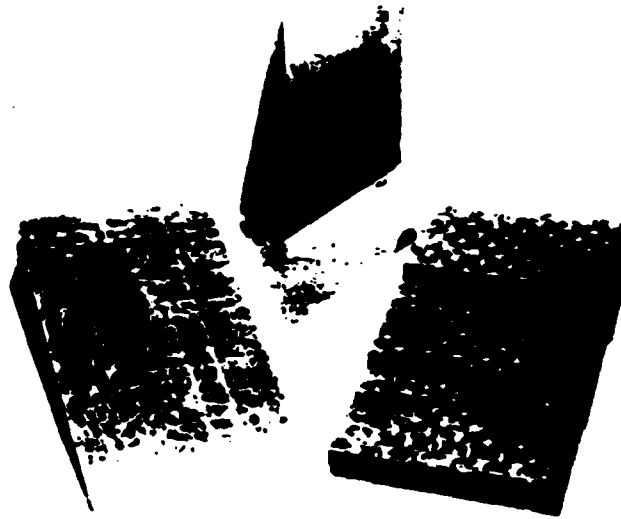


**FIG. 1. Two wedge specimens (epoxy and composite material) and a step specimen (composite material).**

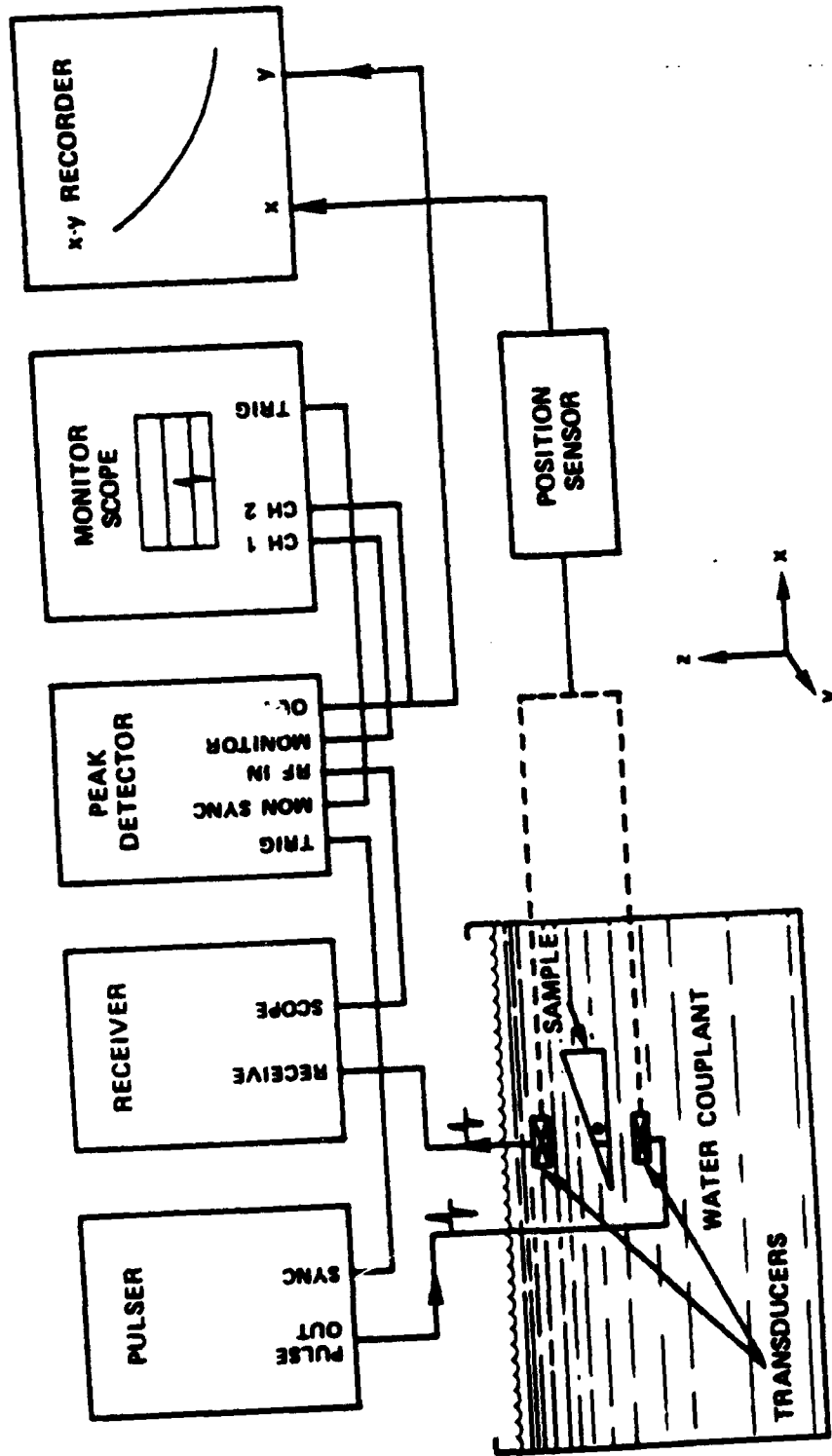


FIG. 2. Experimental set-up for pulse-transmission technique.

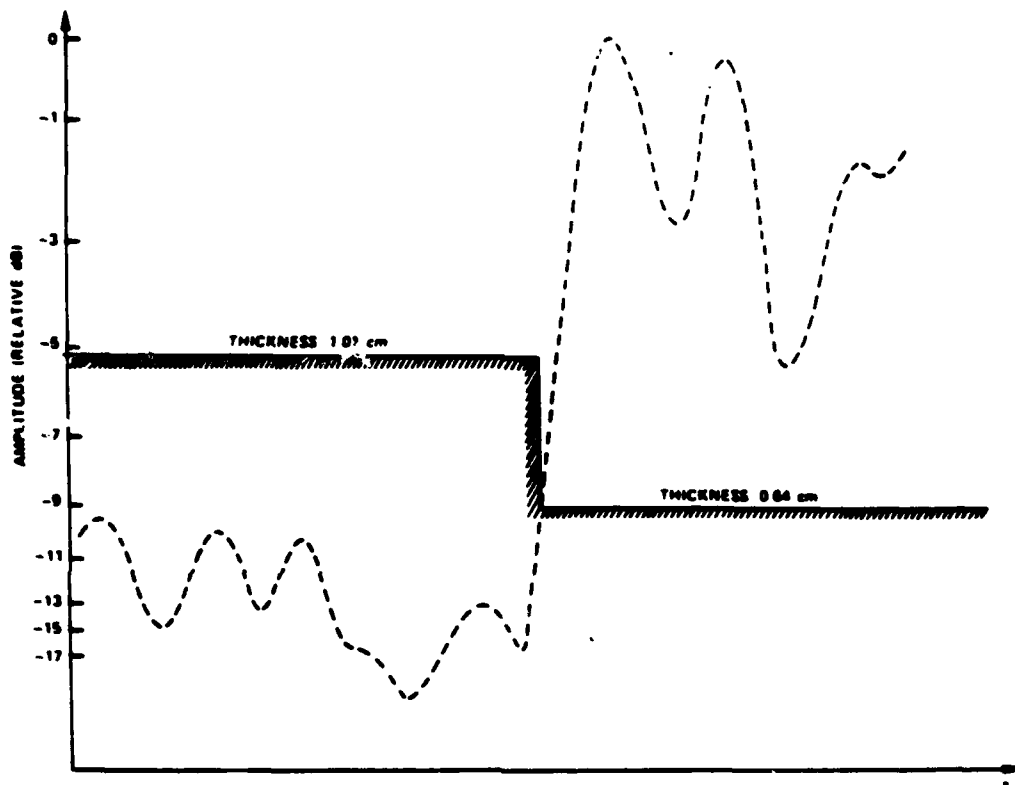


FIG. 3. Attenuation curve for the step specimen.

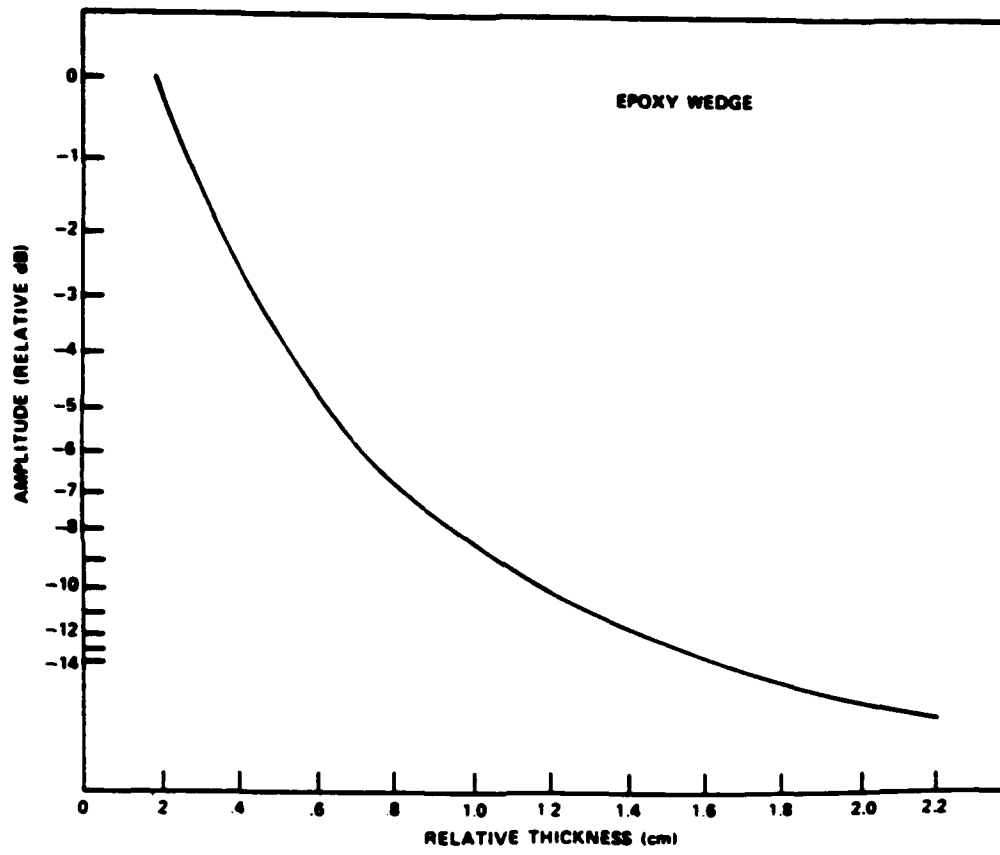


FIG. 4a. Attenuation curve for the epoxy wedge specimen.

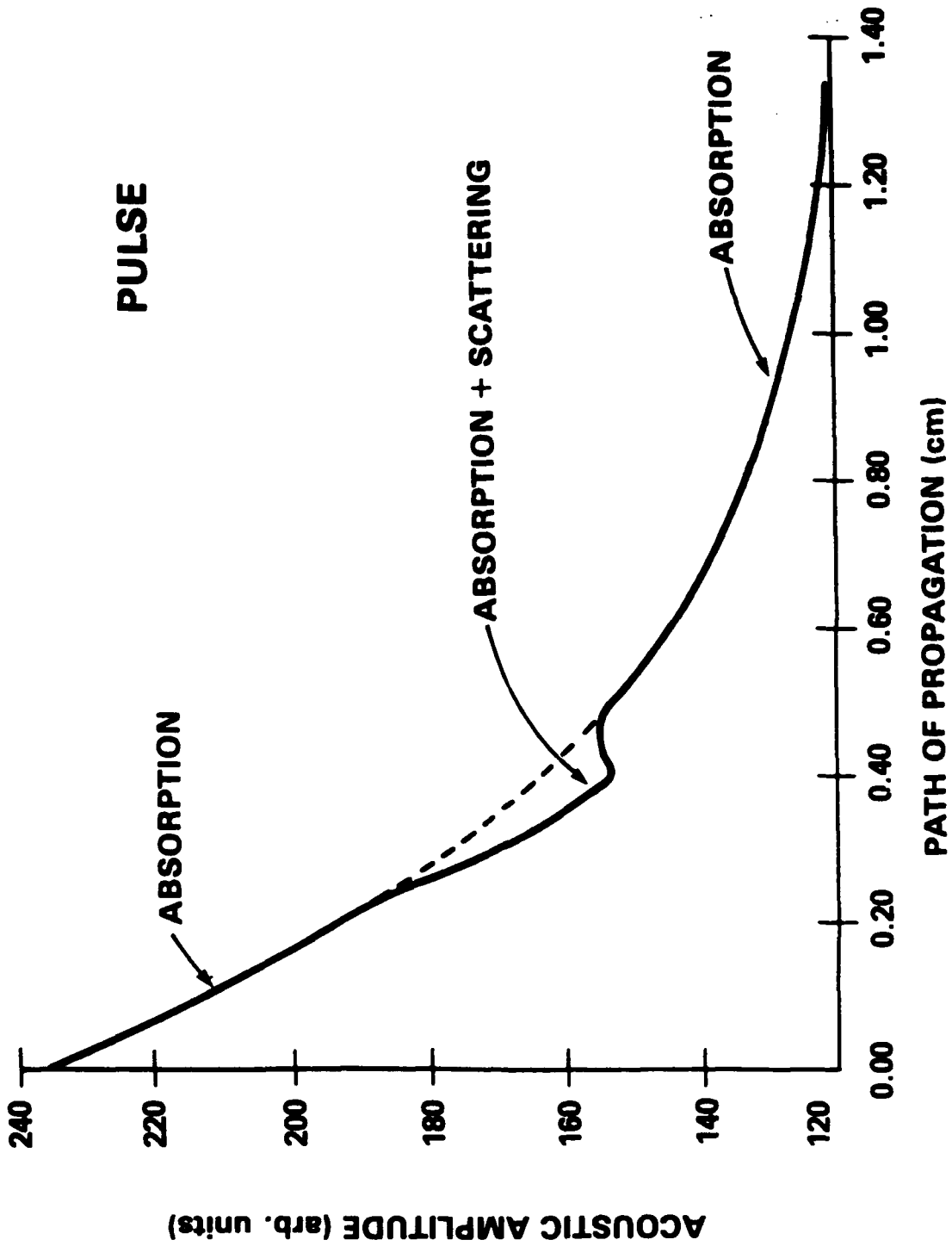


FIG. 4b. Attenuation curve for the epoxy wedge specimen with a flaw.

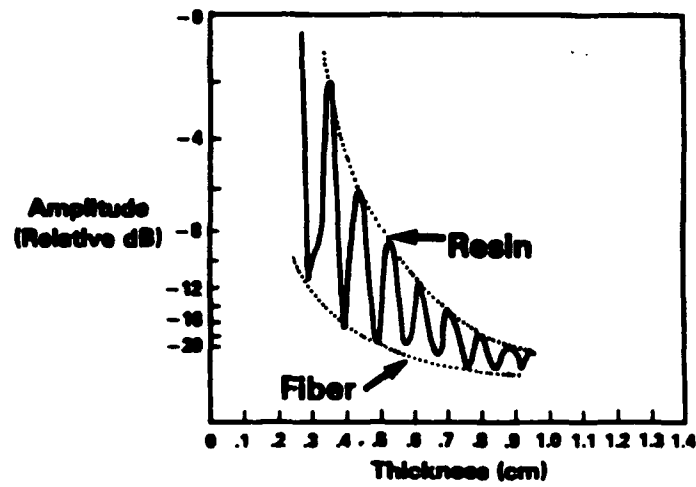


FIG. 5b. Attenuation curve for the flawed regions in the composite wedge specimen.

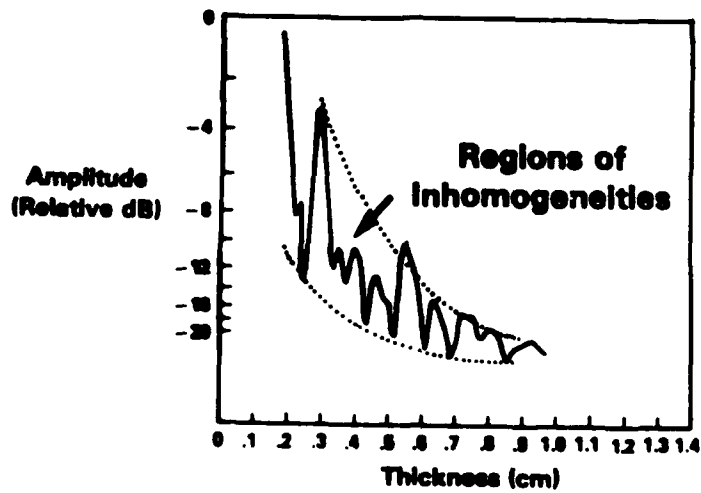


FIG. 5a. Attenuation curve for the unflawed regions in the composite wedge specimen

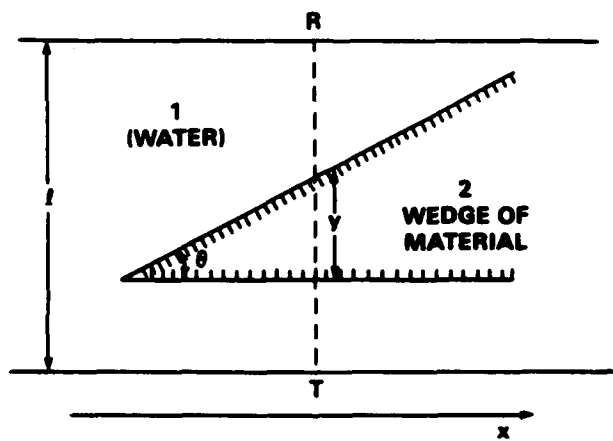


FIG. 6. Arrangement of specimen and transducers (refraction effects ignored).

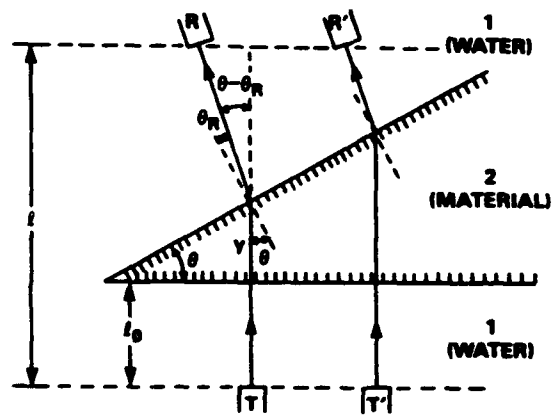


FIG. 7. Arrangement of specimen and transducers (refraction effects included).

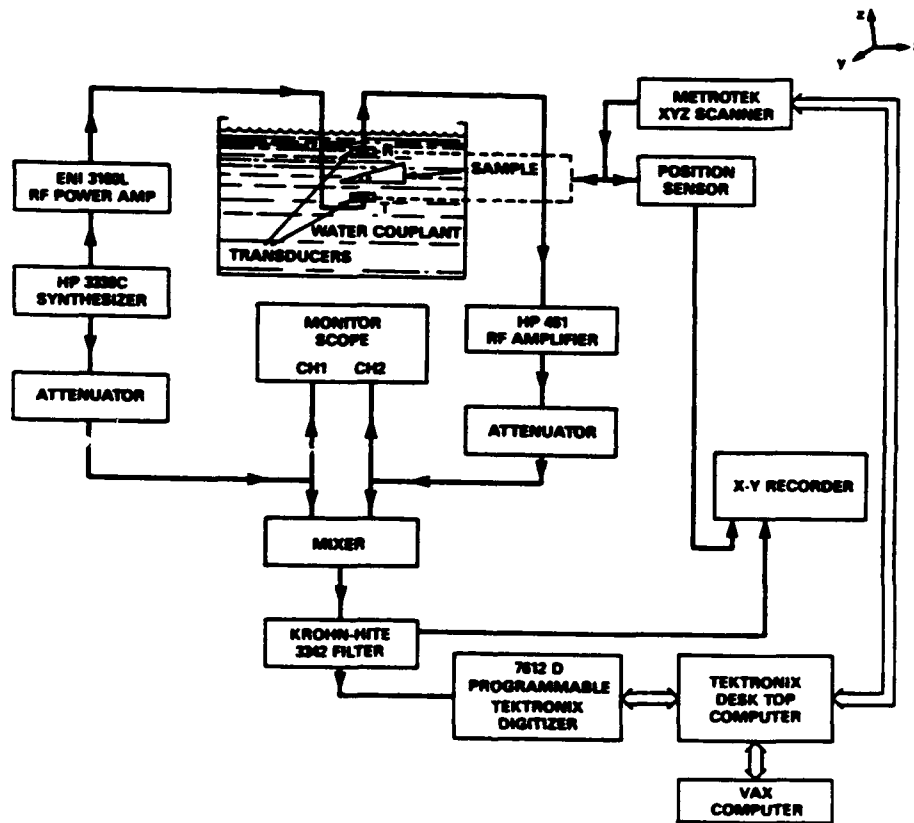


FIG. 8. Experimental setup for ultrasonic interferometric technique.

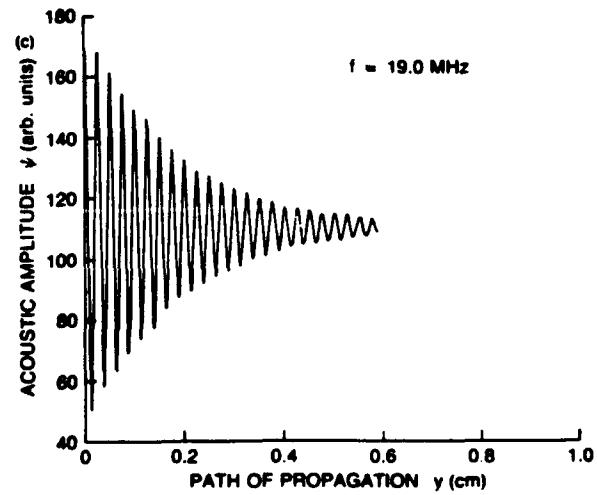
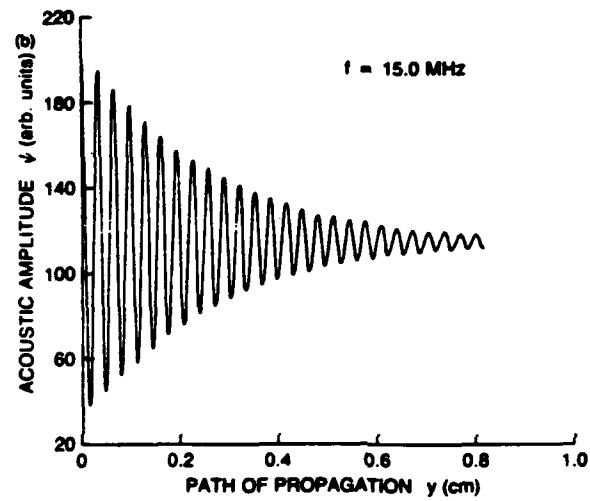
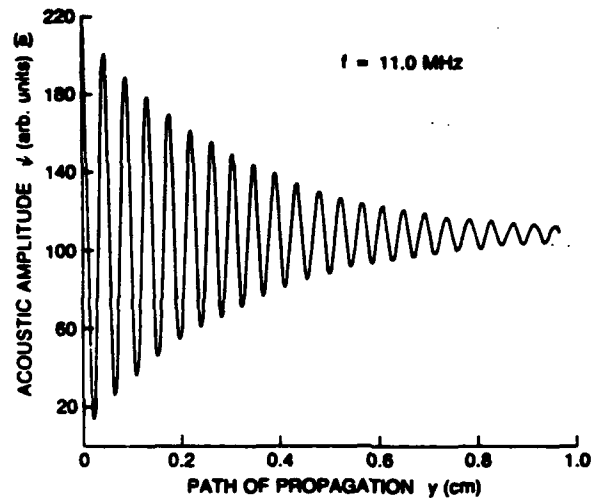


FIG. 9. Typical experimental cross-correlation curves for a specimen without defect at different frequencies: (a) 11 MHz, (b) 15 MHz, and (c) 19 MHz.

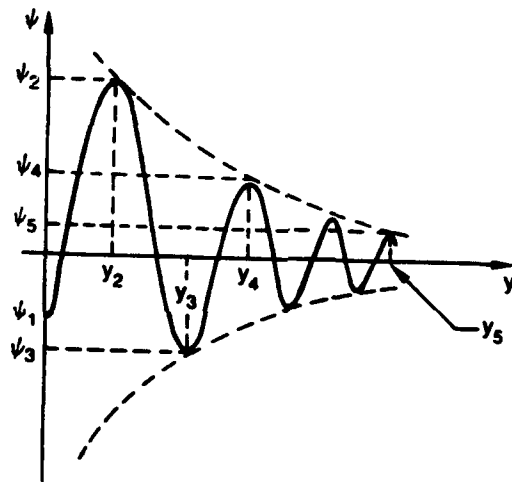


FIG. 10. Graphical representation of the five-point data analysis.

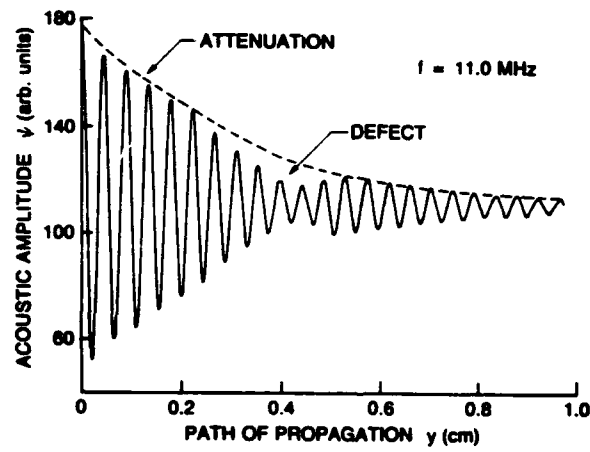
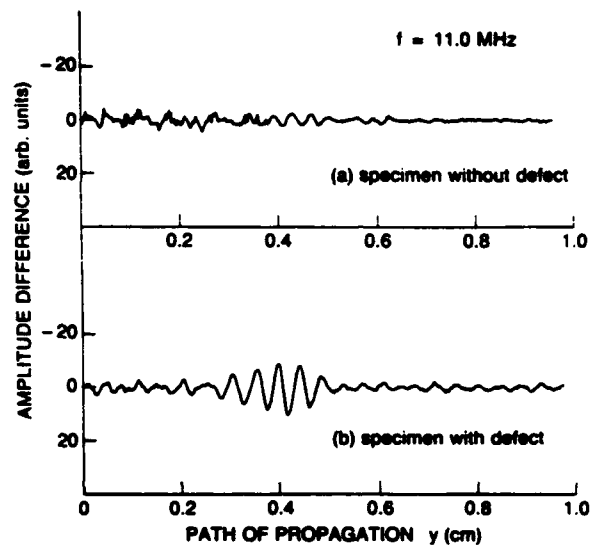


FIG. 11. Cross-correlation curve for a specimen with a hole drilled in it.



**FIG. 12.** Difference between the theoretical least-squares fitted curve and the corresponding experimental curve (a) for a specimen without defect and (b) for a specimen with defect. The signature of the defect is clearly visible.

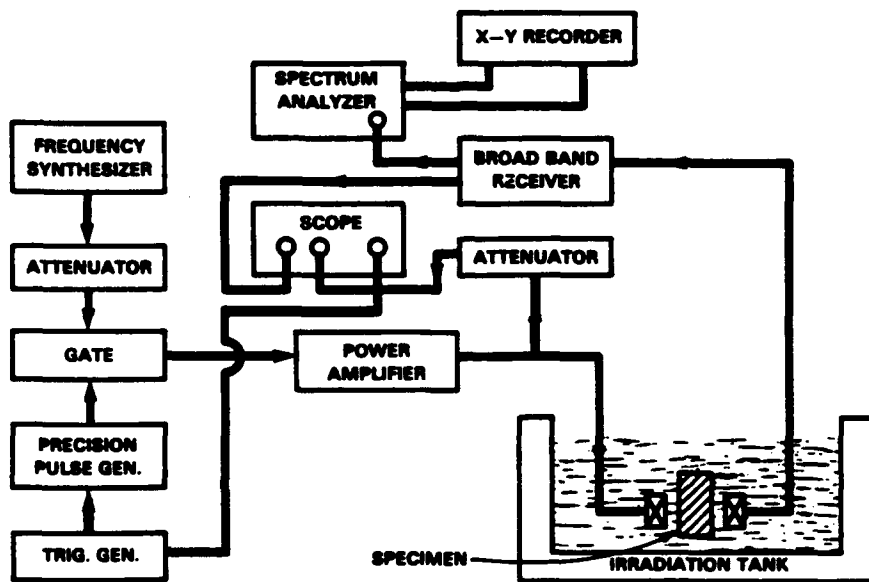


FIG. 13. Experimental set-up for ultrasonic spectral analysis.

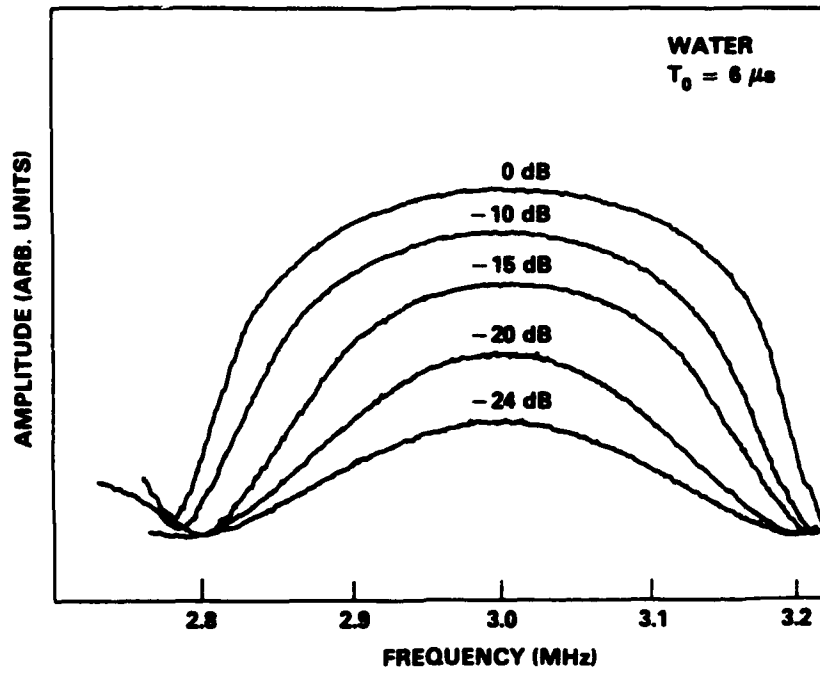


FIG. 14. Spectrum of toneburst propagated through water.

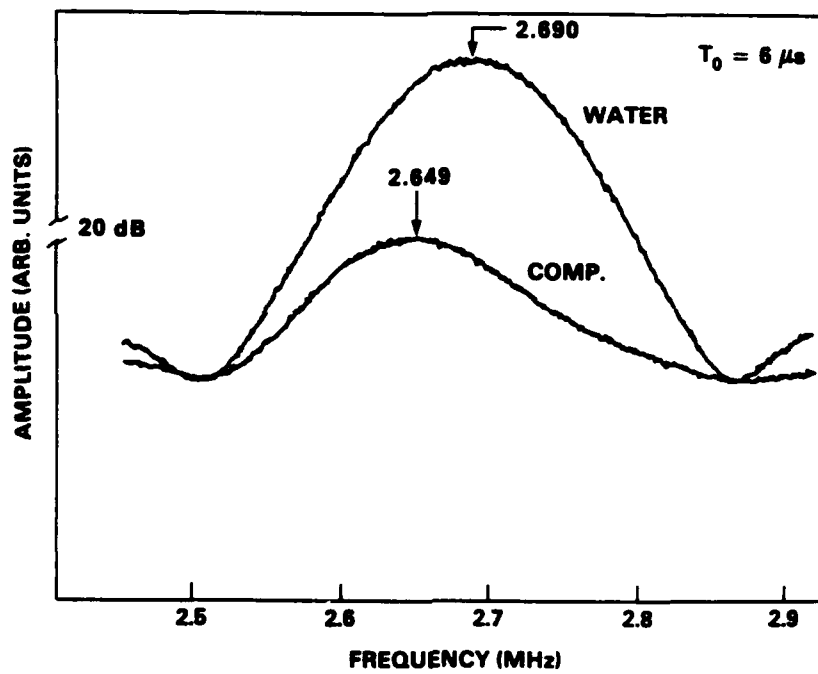


FIG. 15a. Spectrum of toneburst of duration  $6 \mu s$  propagated through composite and water.

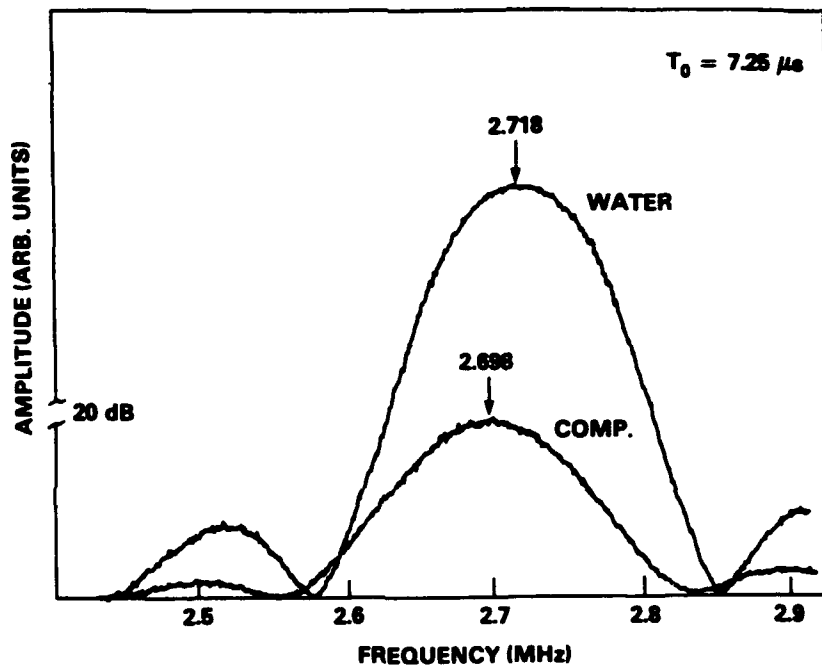


FIG. 15b. Spectrum of toneburst of duration  $7.2 \mu s$  propagated through composite and water.

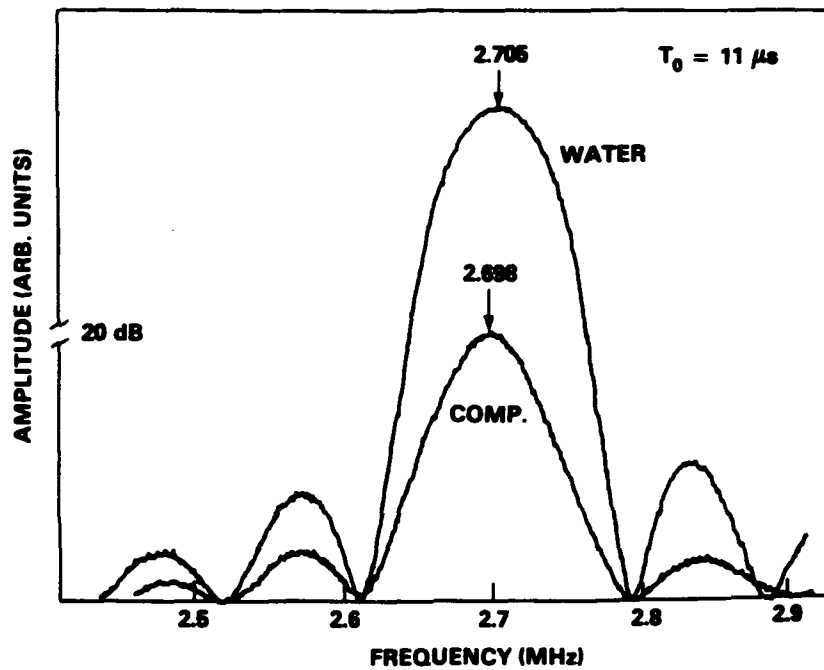


FIG. 15c. Spectrum of toneburst of width  $11 \mu s$  propagated through composite and water